Dianne Benson,[1] *Prasanna Karpur,*[1] *David A. Stubbs,*[1] *and Theodore E. Matikas*[1]

Evaluation of Damage Evolution and Material Behavior in a Sigma/Ti-6242 Composite Using Nondestructive Methods

REFERENCE: Benson, D., Karpur, P., Stubbs, D. A., and Matikas, T. E., **"Evaluation of Damage Evolution and Materials Behavior in a Sigma/Ti-6242 Composite Using Nondestructive Methods,"** *Composite Materials: Fatigue and Fracture (Sixth Volume), ASTM STP 1285*, E. A. Armanios, Ed., American Society for Testing and Materials, 1997, pp. 494–515.

ABSTRACT: Correlations between damage, as it evolves under simulated service conditions, and the results produced from nondestructive evaluation (NDE) techniques are useful in establishing successful life prediction methodologies in metal-matrix composites. Traditional characterization techniques provide limited information on the failure mechanisms in metal-matrix composites because of the complexities caused by the inhomogeneous, anisotropic nature of these materials. In addition, the currently used destructive techniques yield only qualitative information on the internal damage of composites. Very little quantitative information exists correlating the internal damage with property changes in the material such as stiffness, elongation, and residual strength. This research effort correlated NDE results with the residual tensile strength of a six-ply, unidirectional BP Sigma-1240 SiC/Ti-6Al-2Sn-4Zr-2Mo composite after being isothermally fatigued. Baseline tension and fatigue curves were initially generated since minimal information on this particular metal-matrix composite was available in the literature. Information obtained from these tests was used to pinpoint load levels and interruption points for subsequent interrupted fatigue tests. The following nondestructive evaluation techniques were used to evaluate the test specimens before and after fatigue testing: (1) scanning acoustic microscopy, (2) oblique incidence shear wave scanning, (3) reflector plate ultrasonic scanning, (4) immersion surface wave scanning, (5) in situ surface and longitudinal waves and, (6) X-ray radiography. Following the interrupted fatigue tests, the composite specimens were nondestructively evaluated again prior to the residual tension tests to determine the residual strength. Scanning electron microscopy and metallography were used in the correlation and verification of fatigue damage. From these results, the immersion surface wave technique proved to be the most promising method for correlating damage with the residual tensile strength for this particular composite. This paper presents the results from each of the NDE techniques and examines the correlation among the techniques, other destructive methods, and the residual tensile strength.

KEYWORDS: nondestructive evaluation, metal-matrix composites, residual tensile strength, isothermal fatigue, scanning acoustic microscopy, oblique incidence shear waves, reflector plate inspection, in situ surface acoustic waves, in situ longitudinal acoustic waves, fatigue (materials), fracture (materials), composite materials

[1]Graduate student, associate professor and research engineer, associate research engineer and associate research engineer, respectively, University of Dayton Research Institute, 300 College Park Ave., Dayton, OH 45469–0126.

Continuous-fiber metal-matrix composites (MMCs) have a multitude of potential applications in situations requiring light-weight, high stiffness materials possessing high temperature capability [*1*]. Some of the potential applications for these materials are high-performance aerospace vehicles, advanced aircraft engines, missiles, advanced supersonic transports, and advanced fighter aircraft [2]. Since all of these applications involve cyclic loads that can lead to a decrease in load carrying capability, frequent inspection and monitoring of these materials for detection and sizing of flaws or other types of damage are necessary to ensure structural integrity [*3,4*].

In the past, information regarding the damage mechanisms occurring in a material was obtained by observing the macroscopic mechanical response of material specimens subjected to forces (static or cyclic), temperatures (static or cyclic), and environments (oxidizing gas, turbine engine exhaust, etc.) representative of the target application. Typical mechanical responses monitored include changes in stiffness, elongation, and residual tensile strength. In addition to the mechanical response, metallographic examination of the material as well as microscopic inspection or photography of the specimen surface were used to reveal oxidation, cracking, or other accumulated damage. These traditional methods proved useful for understanding the propagation of self-similar cracks in both aerospace and automotive structures. In addition, information gained from inspections can be used to determine how often a component needs to be inspected to detect growing cracks before they reach a critical size and cause failure of the structure as a whole [*5*].

Unfortunately, many of the traditional inspection techniques provide somewhat limited information when applied to metal-matrix composites because of the inhomogeneous, anisotropic nature of composites. Damage in the new advanced materials evolves in more subtle forms than a dominant crack that can be quantified primarily through measurements made on the surface of the material. In some tests, a dominant crack is observed on the surface of the composite, but distributed damage can also strongly influence the life of the composite [*6–12*]. A crack can be bridged either by fibers or ductile material that at elevated temperatures can be degraded by environmental attack [*13,14*]. In addition, fibers fail within the material, microcracks form in the matrix [*15,16*], and matrix/fiber debonding occurs. Since these forms of damage are not readily observable or measurable, obtaining information on these typical forms of damage from bulk averaged measurements and other commonly used techniques for established materials is extremely difficult.

Existing nondestructive evaluation (NDE) techniques need to be evaluated, and new experimental capabilities need to be developed to inspect metal-matrix composites and to provide quantitative data because quantitative data is essential for developing methodologies in life prediction studies [*2,9,17*]. A review of the literature revealed only a few studies that quantitatively assessed the residual strength of metal-matrix composites after expending a certain percentage of the proposed fatigue life [*18*]. Therefore, the main objectives of this research effort were to evaluate various NDE methods to study the evolution of isothermal fatigue damage and to correlate this information with the residual strength of the composite. Such correlations between damage, as it evolves under simulated service conditions, and the characterization results from NDE techniques are necessary to produce successful life prediction methodologies.

Background

Nondestructive evaluation methods can be used to evaluate the integrity of a material without compromising its mechanical properties. Each of the NDE techniques used in this study is described in the following paragraphs.

Nondestructive Evaluation Techniques

High-Frequency Scanning Acoustic Microscopy (SAM)—Ultrasonic scanning acoustic microscopy (SAM) is a nondestructive method used for quantifying material elastic properties, detecting surface and subsurface crack initiation and growth, and assessing fiber-matrix interfacial damage [*19*]. Acoustic microscopy uses an ultrasonic beam diameter that is smaller than the fiber diameter allowing for evaluation of microscopic and macroscopic variations. The scanning acoustic microscope was developed by Quate et al. [*20*] for the nondestructive evaluation of integrated circuits [*21*] and has been extensively studied by Briggs et al. [*22,23*]. The primary contrast mechanism in a SAM is the presence of leaky Rayleigh waves that are very sensitive to local mechanical properties of the materials under study. Since the generation and propagation of the leaky Rayleigh waves are affected by the material properties, imaging of even subtle changes of the mechanical properties is possible. The SAM can be used to understand the flaw initiation and growth mechanisms at the surface as well as the subsurface depths when the transducer is suitably defocused. In general, delaminations, fiber/matrix debonds, matrix cracking, bunched fibers, broken fibers, voids, and fiber orientation have been detected and verified using this temperature [*5*]. Materials studies that have used successfully this technique are described in greater detail in literature [*24–27*].

Oblique Incidence Shear Waves—This technique can be used to characterize the fiber-matrix bond rigidity and load transfer efficiency in composites [*21,28*]. This method produces shear wave propagation in the composite through mode conversion of the incident longitudinal energy at the water/composite interface. The use of this particular method has some advantages compared to other NDE techniques. First of all, resolution capabilities are enhanced since the shear wave velocity is lower than the longitudinal wave velocity for a given frequency. Second, a shear wave incident on the interface between the matrix and the fiber applies stresses that are tangential to the fiber circumference. This method has been used in monitoring the deterioration of the fiber-matrix interface due to elevated temperature tests [*5*] and evaluating fiber alignment and porosity levels in a composite [*29*].

Reflector Plate Ultrasonic Scanning—This technique is similar to conventional through-transmission ultrasonic scanning but uses a reflector plate instead of a receiving transducer. During scanning of the test specimen, ultrasonic waves pass through a test specimen to a glass "reflector plate" beneath the specimen. The waves reflect off the plate and then travel through the specimen a second time before returning to the transducer. The transducer is scanned in a raster pattern acquiring data at regularly spaced X, Y locations. The amplitude of the gated, reflected signals are plotted as a function of X and Y locations to produce a C-scan. This technique has been used to screen out defective and improperly made test samples prior to material behavior studies, thus reducing data scatter due to manufacturing defects. Since this technique is sensitive to changes in material density and elastic modulus [*30*], reflection plate inspection has also been used in identifying damage produced during cyclic loading [*31*].

Ultrasonic Surface Waves—Surface wave (or Rayleigh wave) techniques provide a useful, nondestructive evaluation of near-surface material damage. Surface waves can only penetrate the surface of a material to a depth of approximately one wavelength and are extremely sensitive to the presence of small surface or subsurface cracks. Attenuation of the surface wave is dependent upon the amount of scattering caused by cracks, material grains, other surface anomalies, as well as absorption by the material. The change in attenuation and velocity of surface waves can be used as a good indication of possible changes in the surface and subsurface areas of the material due to cracking and property gradients [*32–34*]. Immersion

pulse-echo ultrasonic inspection using surface waves was used during this research effort to produce C-scan-type images of the specimens. In addition, in situ contact surface waves were used, as proposed by MacLellan [*31*], to monitor progressive damage.

X-Ray Radiography—X-ray radiography is based on the differential absorption of penetrating electromagnetic radiation. Unabsorbed X-rays passing through the part produce an image correlating to variations in thickness or density and is recorded on photographic film. In general, radiography can detect only features that have an appreciable thickness in a direction parallel to the radiation beam. The ability to detect planar discontinuities such as cracks depends on proper orientation of the part to obtain the optimum X-ray absorption differences. An advantage of radiography is the ability to detect flaws located well below the surface of the part [*35*]. X-ray radiography was selected for its capability to image fiber alignment and material abnormalities oriented perpendicular to the material surface as well as its potential in detecting cracks oriented parallel to the X-ray beam. X-ray radiography has been used successfully to detect fiber swimming and misalignment in MMCs [*30*].

Materials and Equipment

Material

The material system evaluated during this study consists of unidirectional BP Sigma SM-1240 silicon carbide (SiC) fibers in a Ti-6Al-2Sn-4Zr-2Mo matrix. The six-ply composite was manufactured by Howmet[2] and was determined to have a fiber volume percentage of 24.5 ± 0.2%. Sigma SM1240 is a C/TiB_2 coated SiC fiber produced by BP Metal Composites Ltd.[3] The SiC is chemical vapor deposited onto a tungsten filament substrate. The fiber has a nominal diameter of 100 μm (0.004 in.), and the duplex protective coating is approximately 2 μm thick. Due to the poor thermal shock resistance of the outer TiB_2 coating, which causes fiber degradation during composite manufacture, Howmet developed a protective coating for the fiber to reduce this problem. The matrix material, Ti-6Al-2Sn-4Zr-2Mo, is described as a near-α $\alpha + \beta$ alloy that has good mechanical heat resistance [*36*].

The composite was produced by plasma melting the titanium alloy powder to deposit the matrix material around a fiber array precision wrapped on a mandrel. Monotape layups were produced subsequently by cutting and arranging the fiber-reinforced "monotapes." Multilayered fiber-reinforced composite panels were produced by hot consolidation of monotape layups using hot isostatic pressing. This method reportedly offers the advantage of improved fiber spacing control over conventional methods of titanium-matrix composite (TMC) fabrication [*37*].

Specimens were cut from the consolidated, unidirectional plate by abrasive water jet into dog-bone-shaped test specimens (Fig. 1). All specimens were mechanically tested with the load applied in the longitudinal, or fiber, direction.

Ultrasonic Test Equipment

The ultrasonic data acquisition and imaging system used for reflection plate inspection and immersion surface wave scanning consisted of a five-axis mechanical scanning system with 0.025-mm minimum step size (the actual resolution of the system is dependent on the ultrasonic frequency used and is generally larger than the step size), broadband ultrasonic spike pulser/

[2]Howmet Corporation, Operhall Research Center, Whitehall, MI.
[3]BP Metals Composites, Ltd., Farnborough, UK.

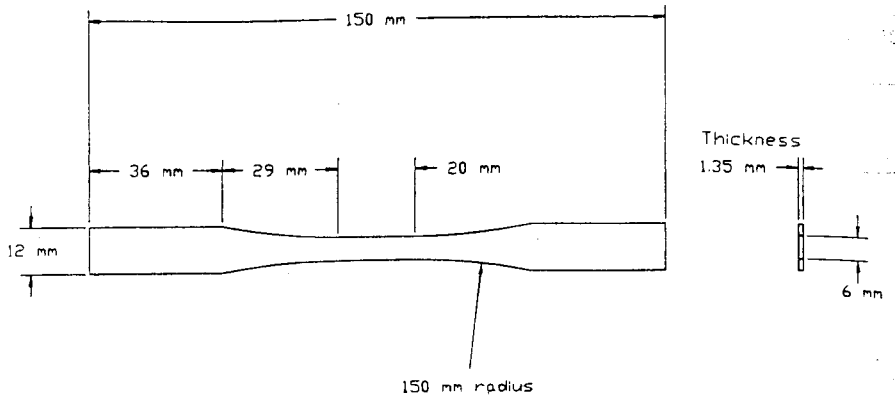

FIG. 1—*Schematic of dog-bone-shaped fatigue specimens used during this study.*

receiver, and a 100-MHz, 8-bit signal digitizer. Data acquisition and imaging were controlled by a computer with custom software. Information about the transducers used during the scans is listed in Table 1. The glass plate used during reflection plate inspection was 18 mm thick.

The ultrasonic data acquisition and imaging system used for oblique incidence shear wave scanning and acoustic microscopy also consisted of a five-axis mechanical scanning system with 0.025-mm resolution. However, the broadband pulser/receiver used had a wider bandwidth and a shorter pulse necessary for high frequency scanning. In addition, a 2-GHz 8-bit digitizer was used. As mentioned previously, data acquisition and imaging were controlled by a digital computer with custom software. Information about the high frequency transducers used during the scans is also listed in Table 1.

Equipment used to generate, receive, and digitize ultrasonic signals during in situ ultrasonic testing consisted of a broadband (35-MHz) ultrasonic spike pulser/receiver and a personal computer equipped with a 100-MHz 8-bit resolution data acquisition board for digitization of the ultrasonic signal [*31*]. Surface wave transducers and wedges were necessary for in situ surface wave monitoring (Fig. 2*a*), and in situ longitudinal wave testing required a fatigue test frame with grips machined specially for placement of the ultrasonic transducers at the ends of the specimens (Fig. 2*b*). Broadband contact transducers possessing a center frequency of 10 MHz were used for both in situ surface wave and longitudinal wave monitoring. Mode conversion wedges were specially manufactured by Panametrics[4] to produce surface waves in titanium matrix composites. The primary couplant used to provide good acoustic coupling

TABLE 1—*Transducer information.*

Scan Type	Transducer Frequency, MHz	Diameter, mm	Focal Length, mm	Theoretical −6dB Focal Spot Size, mm
Immersion surface wave	10	12.7	76.2	0.92
Reflection plate	25	6.35	50.8	0.49
Oblique incidence shear wave	50	6.35	12.7	0.062
Acoustic microscopy	100	6.35	5.08	0.012

[4]Panametrics, Waltham, MA.

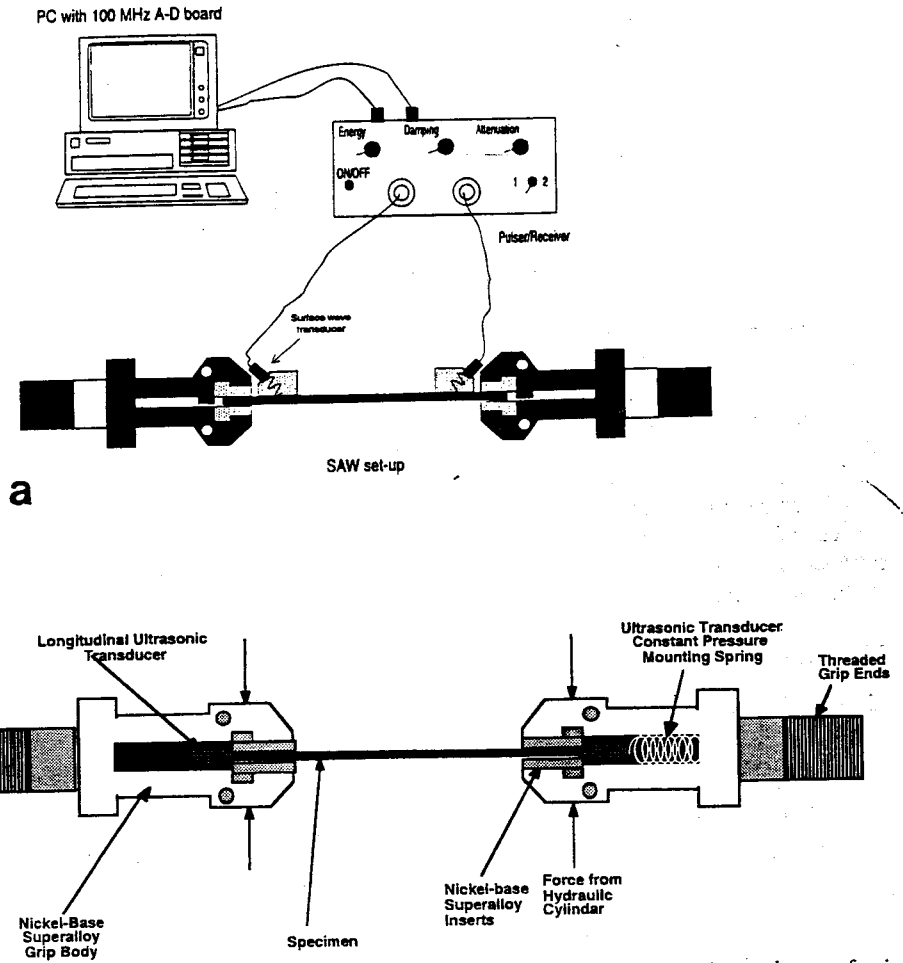

FIG. 2—(a) *Experimental setup for in situ surface wave testing.* (b) *Experimental setup for in situ longitudinal wave testing.*

during testing was Vaseline Petroleum Jelly. It was used because its viscous nature prevents significant evaporation of the couplant over time intervals of 100 h or more. An alternate couplant, THERMOSONIC, a high temperature (0 to 500°F) couplant manufactured by Echo Ultrasound,[5] was used during in situ longitudinal wave characterization. All in situ tests were conducted at room temperature.

A standard film-based X-ray system was used to take the X-ray radiographs. Typical energies were 60 to 80 keV with 5-mA current. Exposure times range from 30 to 60 s, and high-resolution film was used. The system was set up to give a 1:1 specimen-size-to-image—size exposure. Previous work showed that this system could image individual fibers in MMCs [*30*].

[5]Echo Ultrasound, Reedsville, PA.

Mechanical Test Equipment

Isothermal fatigue tests were conducted on a horizontal test frame incorporating a pneumatic ram for load control. The test system was positioned horizontally to improve temperature control and to allow for proper extensometry mounting. A 25-kN load cell was used, and loads were controlled to within 0.1 kN. Specimens were positioned horizontally in precisely aligned, hydraulically actuated, rigid grips [*37–39*]. Gripping pressure was approximately 60 MPa. A symmetric, triangular load cycle was generated by a personal computer using control software developed by the University of Dayton [*40*]. Axial strain was acquired throughout the tests with a 12.7-mm gage length, high-temperature, MTS extensometer containing quartz extension rods.

For the 500°C fatigue tests, the specimens were heated using radiant energy, quartz lamp, heaters. Two heating units were used, each containing four tungsten filament quartz lamps. One heater was positioned above the top surface of the specimen and the other placed below, and each lamp was paired with another to form four controllable heating zones. A uniform temperature profile (±3°C) was maintained throughout a 25-mm region centered along the length of the specimen. The quartz lamp outputs were controlled by commercial four-zone, digital, temperature controllers. Four Type K thermocouples welded to the top and bottom surfaces of the specimen were used for temperature sensing. A more detailed description is provided by Hartman et al. [*37–39*]. This heating system produced a temperature of 500 ± 3°C in the specimen gage section for the duration of the tests.

Procedures

Baseline Tension and Fatigue Tests

Since the literature contains minimal information on the Sigma/Ti-6242 composite system, baseline tension and fatigue curves were generated. Two tension tests were conducted at room temperature, and another two were tested at 500°C. This temperature was chosen since it represents the upper limit at which Ti-6242 is typically used [*36*]. The tests were run in load control at a rate of 10 MPa/s. Information obtained from these tests was used in the selection of load levels and interruption points for subsequent fatigue tests.

Baseline isothermal fatigue tests were conducted at room temperature and 500°C as depicted in Fig. 3. All tests were tension-tension fatigue, run in load-control with a triangular waveform, a stress ratio of 0.1, and a frequency of 0.01 Hz. Six baseline fatigue tests were conducted at each temperature. The maximum applied stress for each test was chosen as a percentage of the baseline ultimate tensile strength at that temperature: 60, 65, 72, 80, and 90%. The stress ratio was chosen to ensure consistency with previous work done on similar titanium matrix composites, and the frequency was selected to ensure a uniform loading profile since pneumatic-actuated fatigue systems are limited in this regard at higher frequencies.

Interrupted Isothermal Fatigue Tests

The maximum applied tensile stress for all interrupted fatigue tests was 65% of the ultimate tensile stress at the corresponding temperature. This stress level was chosen to yield a fatigue life that did not exceed 10 days due to time constraints. The temperatures, frequencies, and stress ratios were consistent with the baseline tests. Baseline curves, changes in modulus, and in situ surface wave data were all used in the selection of appropriate interruption points for each specimen. The interruption points relative to fatigue lives of baseline specimens tested at the same stress level are shown in Fig. 4. The in situ surface wave technique was used to monitor progressive damage throughout the room temperature tests [*31*]. Some of the room

STRESS (MPa)

FIG. 3-
and 500°

STRESS (MPa)

FIG.
study.

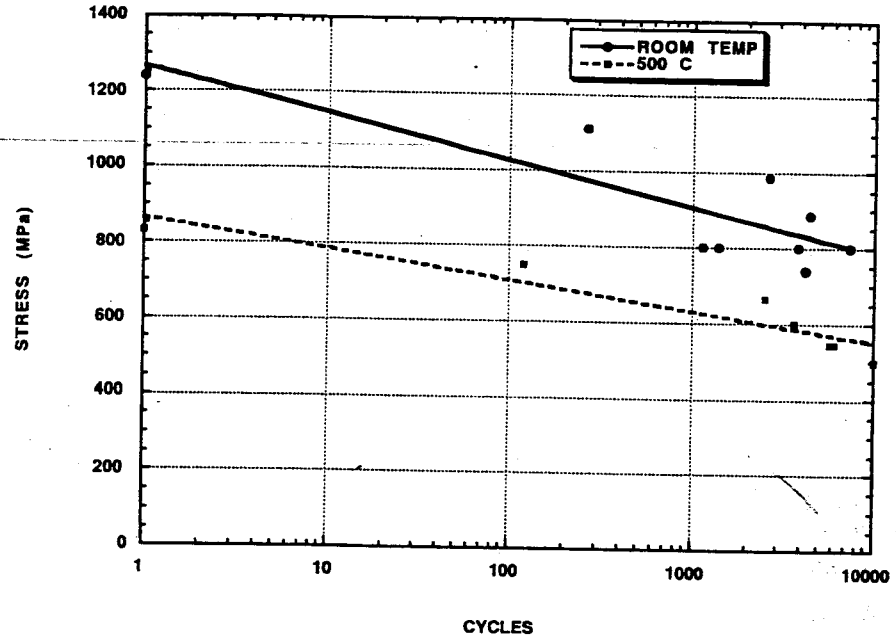

FIG. 3—*Baseline isothermal fatigue curves for Sigma/Ti-6242 composite at room temperature and 500°C (frequency = 0.01 and H_2/R = 0.1).*

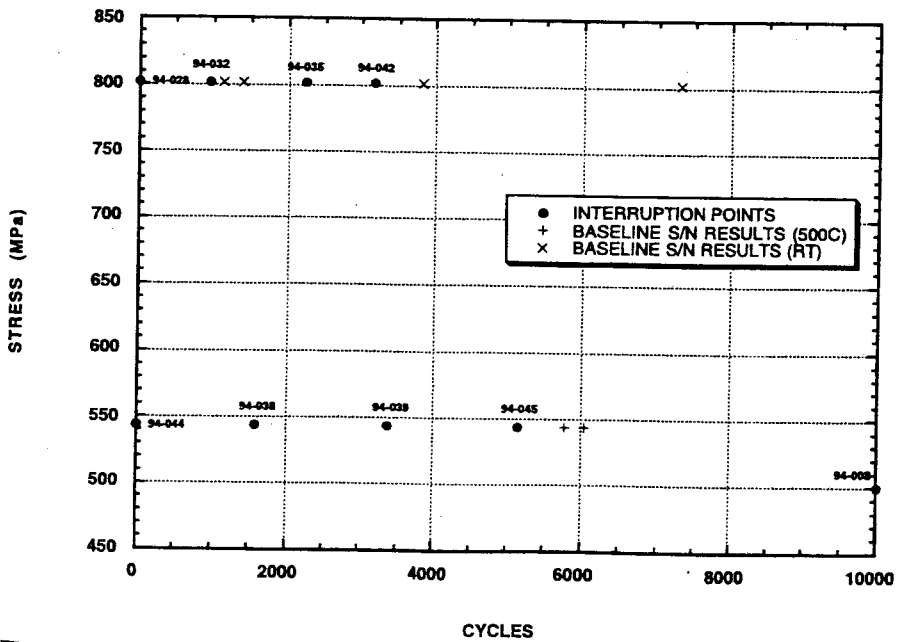

FIG. 4—*Cycles accumulated prior to interruption or failure for fatigue specimens used in this study.*

temperature specimens were interrupted during testing, ultrasonically C-scanned in immersion tanks, and then reinstalled in the fatigue fixture for additional cycling if minimal damage was evident.

One isothermal fatigue test was conducted at room temperature to monitor longitudinal waves traveling the length of the specimen. A horizontal, servohydraulic test frame with specially machined grips for placement of the contact transducers at the ends of the specimen (Fig. 2*b*) was used. This test was tension-tension fatigue, run in load-control with a triangular waveform at a stress ratio of 0.1 and a frequency of 1 Hz. As with the interrupted fatigue tests, the maximum applied tensile stress was 65% of the ultimate tensile strength.

Nondestructive evaluation of the interrupted specimens was performed to characterize damage such as matrix cracking, fiber bridging, or cracked fibers. The following methods were used to evaluate each specimen before and after fatigue testing: high-frequency scanning acoustic microscopy, oblique incidence shear waves, reflector plate ultrasonic scanning, immersion surface waves, and X-ray radiography.

Following the nondestructive evaluation of the test specimens, tension tests were conducted to determine residual strength. All tests were run in load control at a rate of 10 MPa/s at room temperature.

Failure Analysis

After testing, scanning electron microscopy, metallography, and other destructive methods were used to characterize fatigue damage. Qualitative and quantitative data obtained from fatigue tests, nondestructive evaluations, and residual tension tests were correlated with the observations made during destructive analyses.

Results and Discussion

Feasibility of Nondestructive Techniques for Evaluating Damage Evolution and Material Behavior

Reflector Plate Ultrasonic Scanning—Reflector plate C-scans of Specimen 94-047 at various points in its fatigue life are shown in Fig. 5. This specimen was fatigue tested at room temperature and the testing was interrupted three times during fatigue cycling (1000, 1965, and 3822 cycles at a maximum applied stress of 800 MPa) and ultrasonically scanned (in an immersion tank, off the load frame). The C-scans were calibrated such that the full-scale amplitudes (white in these C-scans) in the color-coded scales represented the level of ultrasonic transmission in a Ti-6-4 specimen of similar thickness. Slight differences in amplitude from one image to the next represent typical variances in the calibration process. Regions of attenuation of the ultrasound oriented perpendicular to the specimen axis are apparent at all stages of testing and do not appear to change significantly during testing. These regions are possibly caused by localized bunching of fibers along the width of the specimen as indicated in Fig. 6 (metallograph of the edge of the sample). Many of the specimens fatigue tested during this study failed adjacent to one of these attenuated regions. No other anomalies were evident in the reflection plate scans.

Immersion Surface Waves—Immersion surface wave scans of room temperature fatigue specimens interrupted prior to failure are shown in Fig. 7. All scans were calibrated such that the full-scale amplitudes (black in these C-scans) in the color-coded scales represent the level of reflection from the polished edge of a Sigma/Ti-6242 calibration block. Attenuation was reduced by 12 dB prior to scanning of the actual specimens to increase detection sensitivity. None of the specimens showed any evidence of surface or subsurface damage prior to testing.

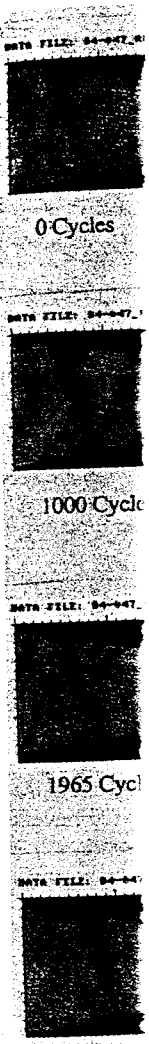

FIG. 5—

However, cr
cycling in S
immersion s
500°C interr
after being i
stress of 50(
exceeding 1
sample reve

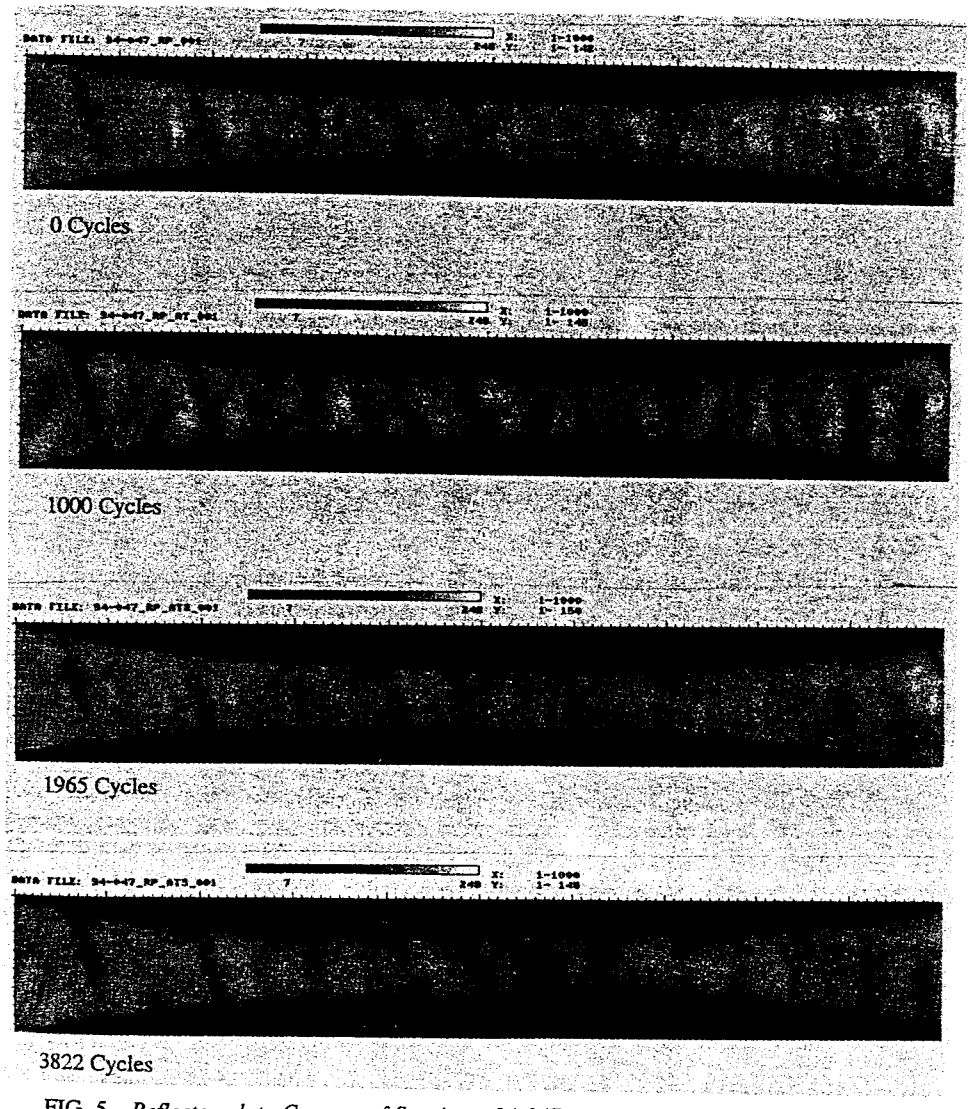

FIG. 5—*Reflector plate C-scans of Specimen 94-047 at various points in its fatigue life.*

However, cracks formed (all the cracks nucleated at the edges) during room temperature fatigue cycling in Specimens 94-035 (2237 cycles) and 94-042 (3168 cycles) as evidenced by the immersion surface wave scans (black regions along the edges of the samples in Fig. 7). The 500°C interrupted fatigue samples, on the other hand, revealed no signs of significant damage after being interrupted. One exception is a 500°C baseline sample tested at a maximum applied stress of 500 MPa. This particular sample (94-008) was removed from the fatigue fixture after exceeding 10 000 cycles due to time constraints. An immersion surface wave scan of this sample revealed several surface and subsurface cracks.

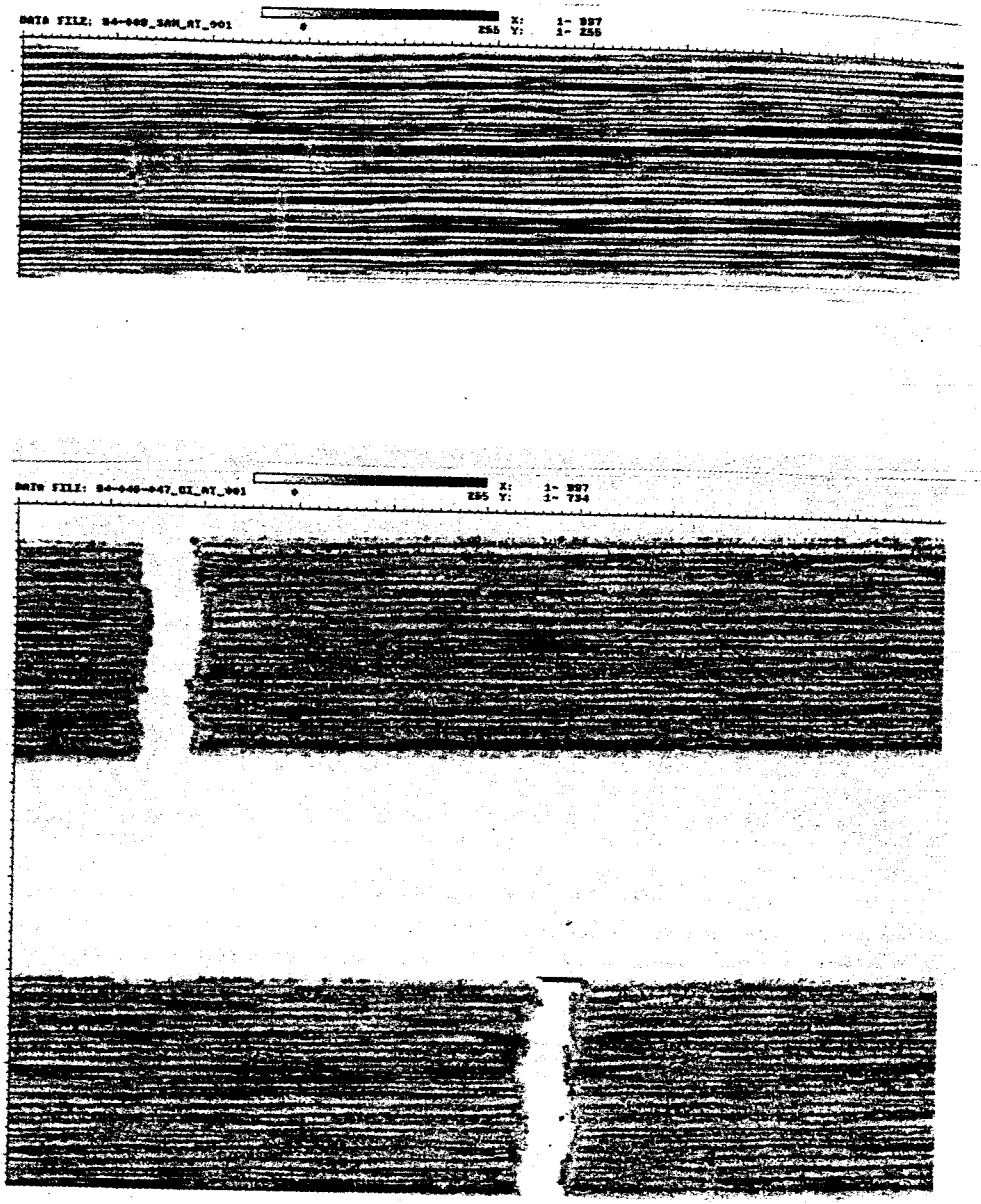

FIG. 9—*Oblique incidence shear wave C-scans of two failed Specimens, 94-046 and 94–047, tested at room temperature.*

transducer frequency was increased to 50 MHz, the wavelength decreased to 92 mm, but attenuation of the shear wave signal increased, which hindered data acquisition. In addition to these difficulties, the undulating nature of the fibers made detection and proper gating of the ultrasonic signal extremely difficult.

In Situ Surface and Longitudinal Waves—In situ surface wave results were similar to those obtained by MacLellan [*31*]. A large, initial decrease of the pitch-catch ultrasonic amplitude was typically seen during the first few cycles and may be an indication of fiber/matrix debonding. Some specimens subsequently displayed an increase in amplitude. This observation was also made by MacLellan [*32*], although the actual cause of the observation is still being investigated at this time. Following this slight increase, the transmitted amplitude gradually decreased until failure occurred. The gradual decrease in surface wave amplitude is believed to be due to reflection and scattering of the ultrasound from damage developing in the material as cycles are applied. A surface wave amplitude plot for Specimen 94-027 is shown in Fig. 10. This specimen, which was cycled at a maximum applied stress of 740 MPa at room temperature, failed after 4191 cycles.

Some difficulties encountered when using this technique may have affected the results. First of all, the transmitted surface wave amplitude was extremely sensitive to slight movements of the wedges. In addition, the potential for error exists during the manual alignment of wedges to maximize the transmitted signal. These practices may have contributed to the variability present in the surface wave amplitude plots of specimens tested under identical conditions. An alignment fixture is recommended for future testing to ensure standardization.

In situ longitudinal wave results for Specimen 94-046 tested at room temperature at a frequency of 1 Hz are shown in Fig. 11 (note the *y*-axis scales). A comparison between changes in longitudinal wave amplitude and modulus (measured using extensometer displacement measurements) yielded similar results; however, the normalized results show that the modulus decreased by about 3% prior to failure, whereas the longitudinal wave amplitude decreased by 17% prior to failure. The longitudinal wave amplitude method is clearly more sensitive to property changes or damage occurring in the material under study, or both.

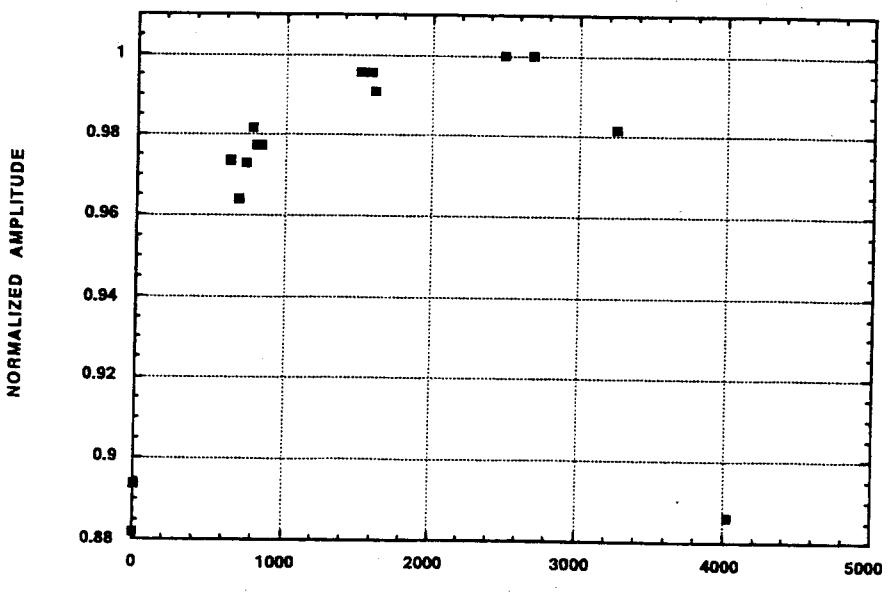

FIG. 10—*In situ surface wave amplitude plot for Specimen 94-027.*

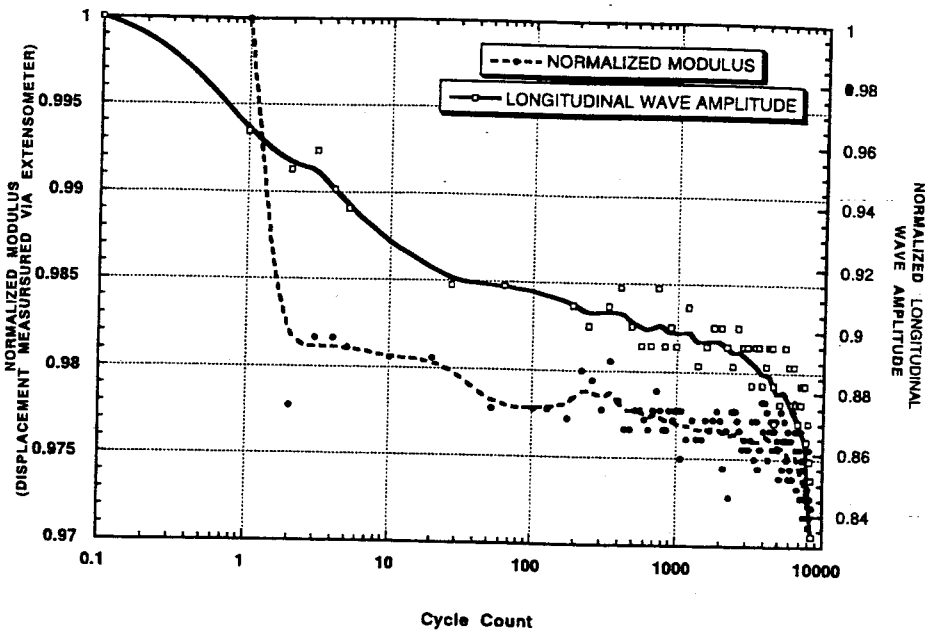

FIG. 11—*In situ longitudinal wave amplitude versus mechanically measured modulus of Specimen 94-046 (65% ultimate tensile strength/room temperature/1 Hz).*

X-Ray Radiography—Regions of low fiber density and fiber displacement were easily detected in the X-ray radiographs taken during this study. Additionally, cracks were apparent in the Sigma/Ti-6242 unidirectional composites using magnification. The cracks were detectable because the fiber breaks appeared as gaps in the tungsten core, and all specimens were unidirectional, which facilitated detection.

Summary—In general, reflector plate method was successful in identifying high fiber density regions caused by bunched fibers. The immersion surface wave technique, on the other hand, succeeded in detecting surface and subsurface cracks. Scanning acoustic microscopy, oblique incidence shear waves, and X-ray radiography were effective in evaluating fiber alignment and some favorably oriented fatigue cracks.

Correlating Observed Damage with Residual Tensile Strength

Table 2 lists the residual tensile strengths and moduli of the interrupted specimens. This information is also shown graphically in Fig. 12. The only specimens showing significant reductions in tensile strength were Specimen 94-035 (2237 cycles), Specimen 94-042 (3168 cycles), and Specimen 94-008 (10 000 cycles). These results correspond well with the findings of the immersion surface wave scans that revealed the presence of surface and sub-surface cracks in these samples. The reduction in tensile strength does not appear to be related to the number of cracks detected; rather, crack size seems to be more indicative of residual tensile strength in this particular composite. Specimens showing no evidence of surface or subsurface cracking possessed residual tensile strengths comparable with the baseline values.

TABLE 2—*Room temperature residual tensile strengths and moduli of interrupted fatigue specimens.*

Specimen	Fatigue Stress, MPa	Temperature, °C	Cycles Accumulated	Residual Tensile Strength, MPa	Mechanically Measured Modulus, GPa
94-030	...	23	0	1243	173
94-048	...	23	0	1226	180
94-028	800	23	1	1317	188
94-032	800	23	955	1213	180
94-035	800	23	2 237	929	178
94-042	800	23	3 168	960	177
94-044	540	500	1	1283	190
94-038	540	500	1 583	1263	182
94-039	540	500	3 369	1273	176
94-045	540	500	5 144	1193	186
94-008	540	500	10 000	759	183

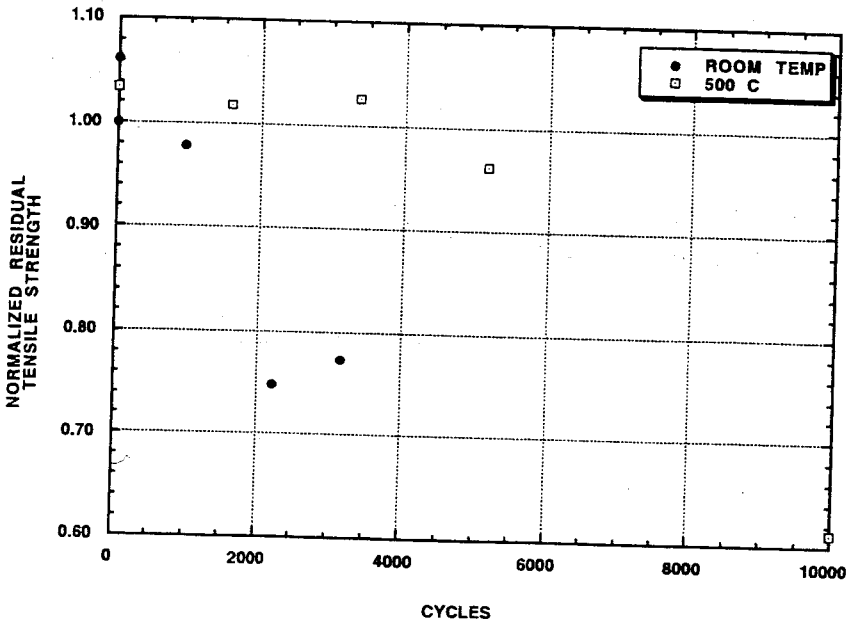

FIG. 12—*Residual tensile strengths of the interrupted fatigue specimens.*

Damage Mechanisms Involved in Producing Indications During Nondestructive Evaluation

Scanning electron microscopy (SEM) of the fracture surfaces of baseline specimens revealed fatigue cracks that initiated at the fiber/matrix interface and propagated radially outward as depicted in Fig. 13. This failure mechanism was detected in both the room temperature and 500°C specimens. Failure of the matrix surrounding some fibers apparently preceded fiber failure and subsequent overload. Fibers near the edges are more susceptible because constraints to failure are reduced once the matrix crack reaches an edge. Metallographic analyses of

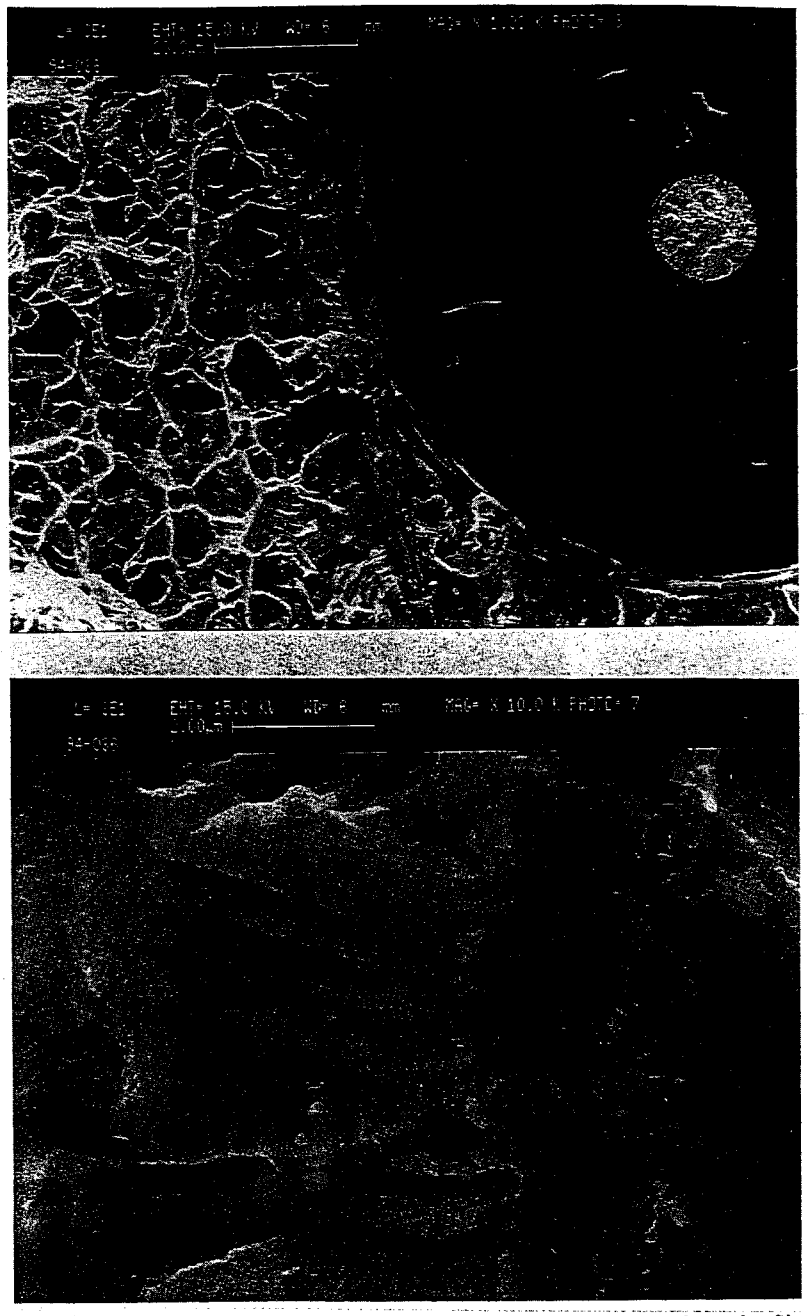

FIG. 13—*Fractographs of Specimen 94-036 showing fatigue emanating from the fiber/matrix interface.*

damaged regio
away from the
In order to
microscopy an
tension tests. L
that possessed
near the fiber/n
decrease in ter
the fracture su
Specimen 94-(
008 (10 000 c
the outer surfa
also present.
tension tests.

Conclusions

The usefuln
Sigma-1240/T
in situ ultraso
Immersion su
correlating fat

FIG. 14—*at 500°C.*

damaged regions were consistent with SEM findings as shown in Fig. 14. Cracks propagating away from the fiber/matrix interface are evident.

In order to verify damage detected during nondestructive evaluations, scanning electron microscopy and metallography were used to evaluate all interrupted specimens after the residual tension tests. Little, if any, fatigue damage was detected on the fracture surfaces of specimens that possessed a residual tensile strength near 100%. Minimal fatigue damage was observed near the fiber/matrix interface of Specimen 94-045 (5114 cycles, 500°C) that displayed a slight decrease in tensile strength. On the other hand, significant fatigue damage was detected on the fracture surfaces of specimens that displayed a reduction in tensile strength after fatigue: Specimen 94-035 (2237 cycles, RT), Specimen 94-042 (3168 cycles, RT), and Specimen 94-008 (10 000 cycles, 500°C, 500 MPa). Most of the visible fatigue damage was located near the outer surface of the specimens; however, fatigue damage at the fiber/matrix interface was also present. These findings correspond well with the NDE results as well as the residual tension tests.

Conclusions

The usefulness of ultrasonic nondestructive evaluation to assess fatigue damage in a $[0]_6$ Sigma-1240/Ti-6242 composite has been demonstrated through correlation of immersion and in situ ultrasonic data with residual tensile strength for the test conditions used in this study. Immersion surface wave scanning proved to be one of the most promising methods for correlating fatigue damage with the residual tensile strength for the composite used in this

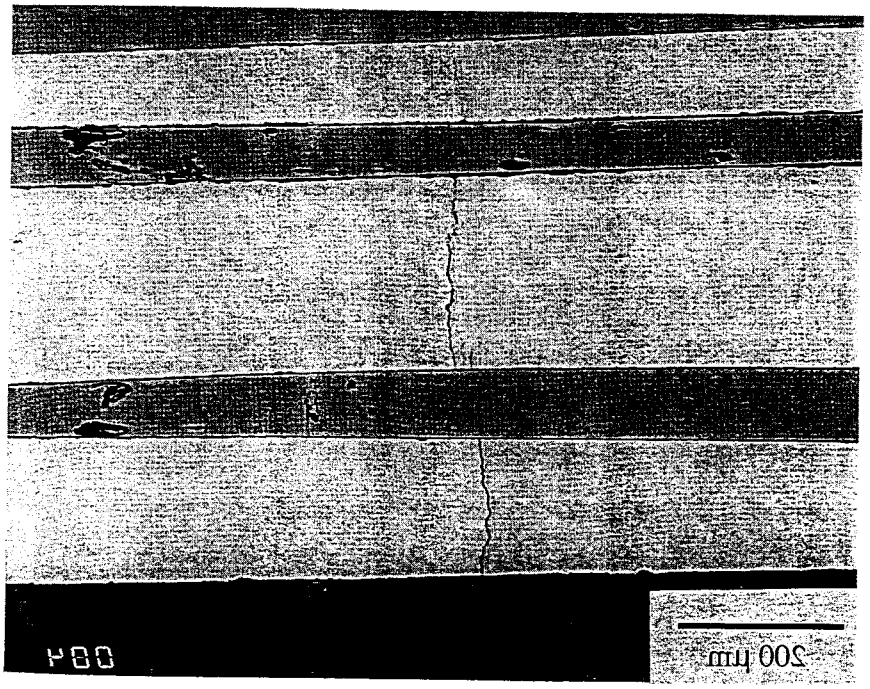

FIG. 14—*Microphotograph showing cracks present in Specimen 94-029 following fatigue failure at 500°C.*

from the fiber/matrix

study as summarized in Tables 3 and 4. The only interrupted specimens showing significant reductions in tensile strength were those found to contain surface or subsurface cracks during scanning. Acoustic microscopy, oblique incidence shear wave, and X-ray radiography techniques proved to be useful in evaluating fiber displacement and locating favorably oriented cracks. Although reflection plate inspection was unsuccessful in identifying damage produced during cyclic loading, slight variations in fiber density due to fiber bunching were detected prior to mechanical testing. In situ surface wave and longitudinal wave methods appeared to be more sensitive to property changes or damage or both occurring in the material than the mechanically measured modulus. Scanning electron microscopy and metallography were used

TABLE 3—*Correlation of immersion surface wave results with residual tensile strength.*

Specimen	Fatigue Stress, MPa	Temperature °C	Total of Number of Fatigue Cycles	Residual Tensile Strength, MPa	Number of Cracks Detected in Gage Section	Maximum Crack Length, mm (Side A + Side B)	Σ Crack Lengths, mm (Side A + Side B)
94-028	800	23	1	1317	0	0	0
94-032	800	23	955	1213	0	0	0
94-035	800	23	2 237	929	4	1.9	4.6
94-042	800	23	3 168	960	8	1.3	3.4
94-044	540	500	1	1283	0	0	0
94-038	540	500	1 583	1263	0	0	0
94-039	540	500	3 369	1273	0	0	0
94-045	540	500	5 144	1193	0	0	0
94-008	540	500	10 000	759	10	2.4	11.9

TABLE 4—*Summary of defects and damage revealed by nondestructive evaluation.*

NDE Technique	Indications Revealed by Technique	Relevant Specimens
Reflector plate	high density regions	all
Immersion surface wave	surface and subsurface fatigue cracks	94-035, 94-042 94-008
Oblique incidence shear wave	fiber alignment in the first ply	all
	surface fatigue cracks >1 mm in length	94-008, 94-047
Scanning acoustic microscopy	fiber alignment in the first ply (touching or bunched fibers, missing fibers)	all
	surface fatigue cracks	94-042, 94-008
	fiber breaks	94-042
In situ surface waves	decrease in pitch catch ultrasonic amplitude may be indicative of damage developing in material	94-027, 94-032, 94-035, 94-042, 94-047
In situ longitudinal waves	sensitive to property changes and/or damage occurring in the material under study	94-046
X-ray radiography	regions of low and high fiber density	all
	displaced fibers	94-030
	fatigue cracks containing cracked fibers	94-035, 94-042, 94-008
Fluorescent penetrant inspection	surface breaking cracks	94-035 94-042 94-008

to verify fatigue damage detected using these methods. Information obtained from nondestructive evaluations has been used to facilitate early detection of damage during fatigue testing of MMCs. However, it should be noted that the damage types and mechanisms in MMCs will vary for different types of cyclical loading, and, therefore, different types of NDE methods will be suitable to detect these damage types. Further research is essential to bring out the usefulness of each NDE method to detect various types of damages caused by different types of fatigue testing methods.

Acknowledgments

Funding for this project was provided through the Air Force Office of Scientific Research Grant F49620-93-1-0461DEF, program manager, Dr. Walter F. Jones; partial support from Air Force Contracts F33615-91-C-5606 and F33615-94-C-5213. All work was performed in the Materials Directorate, Wright Laboratory, at Wright-Patterson Air Force Base, Ohio.

References

[1] Gabb, T. P., Gayda, J., and MacKay, R. A., "Isothermal and Nonisothermal Fatigue Behavior of a Metal Matrix Composite," *Journal of Composite Materials*, Vol. 24, 1990, pp. 667–686.

[2] Johnson, W. S., "Fatigue of Continuous Fiber Reinforced Titanium Matrix Composites," *Proceedings*, Engineering Foundation Conference, MCE Publications, Santa Barbara, CA, 1991, pp. 357–377.

[3] Nayfeh, A. H., Crane, R. L., and Hoppe, W. C., "Reflection of Acoustic Waves from Water/Composite Interfaces," *Journal of Applied Physics*, Vol. 55, 1984, pp. 685–689.

[4] Larson, J. M., Russ, S. M., and Jones, J. W., "Possibilities and Pitfalls in Aerospace Applications of Titanium Matrix Composites," *Proceedings*, NATO AGARD Conference on Characterization of Fiber Reinforced Titanium Metal Matrix Composites, Bordeaux, France, 1993, pp. 1–21.

[5] Karpur, P., Stubbs, D. A., Matikas, T. E., Blodgett, M. P., and Krishnamurthy, S., "Ultrasonic Nondestructive Characterization Methods for the Development and Life Prediction of Titanium Matrix Composites," *Proceedings*, NATO AGARD Conference on Characterization of Fiber Reinforced Titanium Matrix Composites, Bordeaux, France, 1993, pp. 13–1 to 13–12.

[6] Jira, J. R. and Larsen, J. M., "Crack Bridging Behavior in Unidirectional SCS-6/Ti-24Al-11Nb Composite," *Fatigue '93*, J. P. Bailon, I. J. Dicksons, Eds., Engineering Material Advancement Services Ltd., Ecole Polytechnique, Montreal, Canada, Vol. 2, 1993, pp. 1085–1090.

[7] Castelli, M .G. and Bartolotta, P. E., Jr., "Thermomechanical Testing of High Temperature Composites: Thermomechanical Fatigue (TMF) Behavior of SiC(SCS-6)/Ti 15-3," *Composite Materials: Testing and Design, (Tenth Volume) ASTM STP 1120, G. C. Grimess, Ed.*, American Society for Testing and Materials, Philadelphia, 1992, pp. 70–86.

[8] Neu, R. W. and Roman, I., "Acoustic Emission Monitoring of Damage in Metal Matrix Composites Subjected to Thermomechanical Fatigue," *Composites Science and Technology*, Vol. 52, 1994, pp. 1–8.

[9] Neu, R. W., "A Mechanistic Thermomechanical Fatigue Life Prediction Model for Metal Matrix Composites," *Fatigue and Fracture of Engineering Materials and Structures*, Vol. 16, 1993, pp. 811–828.

[10] Russ, S. M., Rosenberger, A. H., and Stubbs, D. A., "Isothermal Fatigue of a SCS-6/Ti- 22Al-23Nb Composite in Air and Vacuum," *Proceedings*, ASME Summer Annual Meeting, American Society of Mechanical Engineers, New York, 1995.

[11] Johnson, W. S., "Mechanisms Controlling Fatigue Damage Development in Continuous Fiber Reinforced Metal Matrix Composites," *Advances in Fracture Research-ICF7*, K. Salama, K. Ravi-Chandar, D. M. R. Taplin, P. R. Raos, Eds., Pergamon Press, New York, 1989, pp. 897–905.

[12] Chan, K. S. and Davidson, D. L., "Fatigue Crack Growth in Fiber-Reinforced Metal-Matrix Composites," *Fatigue of Advanced Materials*, 1990.

[13] Nicholas, T. and Russ, S. M., "Elevated Temperature Fatigue Behavior of SCS-6/Ti-24Al-11Nb," *Material Science Engineering*, Vol. A153, 1992, pp. 514–519.

[14] Kortyna, B. R. and Ashbaugh, N. E., "Fatigue Characteristics of a Titanium Aluminide Composite at Elevated Temperature," *Titanium Aluminide Composites—Proceedings from Titanium Aluminide Composite Workshop*, P. R. Smith, S. J. Balsone, and T. Nicholass, Eds., Report No. WL-TR-91-4020, Wright Laboratory/Wright Patterson AFB, OH, 1991.

[15] John, R. and Ashbaugh, N. E., "Fatigue Crack Growth in Ceramics and Ceramic Matrix Composites," *Cyclic Deformation, Fracture, and Nondestructive Evaluation of Advanced Materials, ASTM STP 1157*, M. R. Mitchell and O. Bucks, Eds., American Society for Testing and Materials, Philadelphia, 1992, pp. 28–51.

[16] Butkus, L. M., Holmes, J. W., and Nicholas, T., "Thermomechanical Fatigue Behavior of a Silicon Carbide Fiber-Reinforced Calcium Alluminosilicate Composite," *Journal*, American Ceramic Society, Vol. 76, 1993, pp. 2817–2825.

[17] John, R., Jira, J. R., and Ashbaugh, N. E., "Analysis of Bridged Fatigue Cracks in Unidirectional SCS-6/Ti-24Al-11Nb Composite," *Fatigue '93*, J. P. Bailon and I. J. Dicksons, Eds., Engineering Material Advancement Services Ltd., Ecole Polytechnique, Montreal, Canada, Vol. 2, 1993, pp. 1091–1096.

[18] Castelli, M. G., *Life Prediction Methodology for Titanium Matrix Composites, ASTM STP 1253*, W. S. Johnson, J. M. Larsen, and B. N. Cox, Eds. American Society for Testing and Materials, Philadelphia, 1995, pp. 412–431.

[19] Karpur, P., Matikas, T. E., and Blodgett, M. P., "Acoustic Microscopy as a Tool for Fiber-Matrix Interface Evaluation," *Proceedings*, First International Conference on Composites Engineering (ICCE/1), New Orleans, D. Huis, Ed., 1994, pp. 253–254.

[20] Quate, C. F., Atalar, A., and Wickramasinghe, H. K., "Acoustic Microscopy with Mechanical Scanning—A Review," *Proceedings*, Institute of Electrical and Electronic Engineers, Inc., New York, Vol. 67, 1979, pp. 1092–1114.

[21] Karpur, P., Matikas, T., and Krishnamurthy, S., "Matrix-Fiber Interface Characterization in Metal Matrix Composites Using Ultrasonic Imaging of Fiber Fragmentation," *Proceedings*, American Society for Composites, Seventh Technical Conference, Technomic, Lancaster, PA, 1992, pp. 420–427.

[22] Briggs, G. A. D., *Acoustic Microscopy*, Oxford University Press, Oxford, 1992.

[23] Lawrence, C. W., Briggs, G. A. D., Scruby, C. B., and Davies, J. R. R., "Acoustic Microscopy of Ceramic-Fibre Composites; Part I: Glass-matrix Composites," *Journal of Materials Science*, Vol. 28, 1993, pp. 3635–3644.

[24] Bertoni, H. L., "Raleigh Waves in Scanning Acoustic Microscopy," *Raleigh Wave Theory and Application*, The Royal Institution, London, Vol. 2, 1985, pp. 274–290.

[25] Blatt, D., Karpur, P., Matikas, T. E., Blodgett, M. P., and Stubbs, D. A., "Elevated Temperature Degradation and Damage Mechanisms of Titanium Based Metal Matrix Composites," *Proceedings*, American Society for Composites, Eight Technical Conference on Composite Materials, Cleveland, 1993.

[26] Blodgett, M. P., Matikas, T. E., Karpur, P., Jira, J. R., and Blatt, D., "Ultrasonic Evaluation of Fiber-Matrix Interfacial Degradation of Titanium Matrix Composites Due to Temperature and Mechanical Loading," 20th Annual Review of Progress in Quantitative Nondestructive Evaluation, Vol. 13B, D. O. Thompson and D. E. Chimentis, Eds., Plenum, Bowdoin College, Brunswick, ME, 1993, pp. 1213–1219.

[27] Karpur, P., Matikas, T. E., Blodgett, M. P., Jira, J. R., and Blatt, D., in *Special Applications and Advanced Techniques for Crack Size Determination, ASTM STP 1251*, J. J. Ruschau and J. K. Donald, Eds., American Society for Testing and Materials, Philadelphia, 1995, pp. 130–146.

[28] Matikas, T. E. and Karpur, P., "Ultrasonic Reflectivity Technique for the Characterization of Fiber-Matrix Interface in Metal Matrix Composites," *Journal of Applied Physics*, Vol. 74, 1993, pp. 228–236.

[29] Bashyam, M., "Ultrasonic NDE for Ceramic- and Metal-Matrix Composite Material Characterization," *Review of Progress in Quantitative Nondestructive Evaluation*, Vol. 10B, D. O. Thompson and D. E. Chimentis, Eds., Plenum Press, New York, 1991, pp. 1423–1430.

[30] Stubbs, D. A. and Russ, S. M., "Examination of the Correlation Between NDE-Detected Manufacturing Abnormalities and Thermomechanical Fatigue Life," *Proceedings*, Structural Testing Technology at High Temperature—II, Society for Experimental Mechanics, Inc., Ojai, CA, 1993, pp. 165–173.

[31] MacLeallan, P. T., Master's thesis, University of Dayton, 1993.

[32] Testa, A. J. and Burger, C. P., "A Measurement of Crack Depth by Changes in the Frequency Spectrum of a Rayleigh Wave," *Proceedings*, Novel NDE Methods for Materials, B. B. Raths, Ed., Metallurgical Society of AIME, 1982, pp. 91–108.

[33] Karpur, P. and Resch, M. T., in *Review of Progress in Quantitative Nondestructive Evaluation*, Vol. 10A, D. O. Thompson and D. E. Chimenti, Eds., Plenum Press, New York, 1991, pp. 757–764.

[34] Achenbach, J. D., Fine, M. E., Komsky, I., and McGuire, S., "Ultrasonic Wave Technique to Assess Cyclic-Load Fatigue Damage in Silicon-Carbide Whisker Reinforced 2124 Aluminum Alloy Composites," *Cyclic Deformation, Fracture and Nondestructive Evaluation of Advanced Materials,*

ASTM STP 1157, M. R. Mitchell and O. Bucks, Eds., American Society for Testing and Materials, Philadelphia, 1992, pp. 241–250.

[35] Deiter, G., *Engineering Design: A Materials and Processing Approach*, McGraw-Hill Book Co., New York, 1983.

[36] *The Physical Metallurgy of Titanium Alloys*, E. W. Collins, Ed., American Society for Metals, Metals Park, OH, 1984.

[37] Hartman, G. A., Zawada, L., and Russ, S., "Techniques for Elevated Temperature Tensile Testing of Advanced Ceramic Composite Materials," *Proceedings*, Fifth Annual Hostile Environment and High Temperature Measurements Conference, Society for Experimental Mechanics, Costa Mesa, CA, 1988, pp. 31–38.

[38] Hartman, G. A. and Russ, S., "Techniques for Mechanical and Thermal Testing of Ti_3Al/SCS-6 Metal Matrix Composites," *Metal Matrix Composites: Testing, Analysis and Failure Modes, ASTM STP 1032*, W. S. Johnson, Ed., American Society for Testing and Materials, Philadelphia, 1989, pp. 43–53.

[39] Hartman, G. A. and Buchanan, D. J., "Methodologies for Thermal and Mechanical Testing of TMC Materials," AGARD Report 796, NATO AGARD Characterization of Fiber Reinforced Titanium Matrix Composites Bordeaux, France, 1993, pp. 12–1 to 12–9.

[40] Hartman, G. A. and Ashbaugh, N. E., "A Fracture Mechanics Test Automation System for a Basic Research Laboratory," *Applications of Automation Technology to Fatigue and Fracture Testing, ASTM STP 1092*, A. A. Braun, N. E. Ashbaugh, and F. M. Smith, Eds., American Society for Testing and Materials, Philadelphia, 1990, pp. 95–112.

Peer Review Policy

Each paper published in this volume was evaluated by three peer reviewers. The authors addressed all of the reviewers' comments to the satisfaction of both the technical editor(s) and the ASTM Committee on Publications.

The quality of the papers in this publication reflects not only the obvious efforts of the authors and the technical editor(s), but also the work of these peer reviewers. The ASTM Committee on Publications acknowledges with appreciation their dedication and contribution to time and effort on behalf of ASTM.